Measurements of the ^{25}Mg(^{11}B, ^{12}C)^{24}Na and ^{25}Mg(^{11}B, ^{10}Be)^{26}Al proton transfer reactions

P. N. de Faria, R. Lichtenthäler, V. Guimarães, A. Lépine-Szily, and E. A. Benjamim
Departamento de Física Nuclear, Instituto de Física da Universidade de São Paulo, CP 66318, 05315-970 São Paulo, SP, Brazil

G. F. Lima
FACENS, Faculdade de Engenharia de Sorocaba, CP 355, 18001-970, Sorocaba, SP, Brazil

A. M. Moro
Departamento de FAMN, Universidad de Sevilla, Apdo. 1065, E-41080 Sevilla, Spain
(Received 5 April 2006; published 23 August 2006)

Angular distributions for the ^{11}B+^{25}Mg elastic scattering, ^{25}Mg(^{11}B, ^{12}C)^{24}Na proton pickup, and ^{25}Mg(^{11}B, ^{10}Be)^{26}Al stripping reactions have been measured at $E_{^{11}\mathrm{B}} = 35$ MeV. The angular distributions have been analyzed by the distorted-waves Born approximation calculations using the code fresco. The spectroscopic factors for the overlaps $\langle ^{25}\mathrm{Mg}|^{26}\mathrm{Al}\rangle$, $\langle ^{25}\mathrm{Mg}|^{24}\mathrm{Na}\rangle$ for the ground state and excited states of ^{26}Al and ^{24}Na have been obtained and compared to previous measurements and shell-model calculations.

DOI: 10.1103/PhysRevC.74.024604 PACS number(s): 25.70.Hi, 24.10.Eq, 24.50.+g, 27.30.+t

I. INTRODUCTION

Nowadays, reliable spectroscopic information can be obtained from transfer measurements. Powerful computer codes exist [1] that allow distorted-waves Born approximation (DWBA) calculations with recoil and finite range. Effects of the coupling to excited states (Coupled-channels Born approximation; CCBA) as well as the coupling to transfer states in all orders (Coupled Reaction Channels; CRC) can be taken into account, thus testing the validity of the DWBA approach.

In the present work, angular distributions for the ^{11}B+^{25}Mg elastic scattering, ^{25}Mg(^{11}B, ^{12}C)^{24}Na proton pickup, and ^{25}Mg(^{11}B, ^{10}Be)^{26}Al stripping have been analyzed using the computer code fresco [1]. We performed DWBA, CCBA, and CRC calculations for the transfer reactions. To obtain the spectroscopic factors for the $\langle ^{25}\mathrm{Mg}|^{24}\mathrm{Na}\rangle$ and $\langle ^{25}\mathrm{Mg}|^{26}\mathrm{Al}\rangle$ from these transfer reactions it is necessary to know the projetile spectroscopic factors for the $\langle ^{11}\mathrm{B}|^{12}\mathrm{C}\rangle$ and $\langle ^{11}\mathrm{B}|^{10}\mathrm{Be}\rangle$ overlaps. We reanalyzed existing data for the ^{11}B(d, ^{3}He)^{10}Be [2] and ^{11}B(d, n)^{12}C [3] reactions and compared the results with theorectical values from Cohen and Kurath [4]. The spectroscopic factors for the $\langle ^{25}\mathrm{Mg}|^{24}\mathrm{Na}\rangle$ and $\langle ^{25}\mathrm{Mg}|^{26}\mathrm{Al}\rangle$ overlaps have been obtained using the Cohen-Kurath values for the projectile and are compared to those obtained from previous measurements [5–7].

The present mesurements were first motivated to investigate the production rate of the ^{24}Na$^{m}(1^{+}; 0.472)$ and ^{26}Al$^{m}(0^{+}; 0.23)$ isomeric nuclei with half-lives of 20.2 ms and 6.35 s, respectively. These transfer reactions could be used as production reactions for the ^{24}Na^{m} and ^{26}Al^{m} secondary beams using the ^{25}Mg primary beam and ^{11}B target in the future Linear accelerator-Radioactive Ions Beams in Brazil [8] facility. Such beams would allow the investigation of the scattering of two nuclei where the projectile nucleus is in an excited state during the collision. New interesting phenomena such as the projectile acceleration could be observed in these experiments [9–12].

II. EXPERIMENTAL PROCEDURE

The 35 MeV ^{11}B beam was produced by the 8 MV São Paulo Pelletron Tandem accelerator with an intensity of about 300 nAe. The 20 μg/cm^2, ^{25}Mg targets have been manufactured at the Pelletron Laboratory [13] by evaporation of isotopically enriched ^{25}MgO (97%) on a carbon backing of approximately 15 μg/cm^2. A thin layer of 0.2 μg/cm^2 of ^{209}Bi was evaporated on the carbon backing for normalization purposes. The detector system consisted of three telescopes formed by gas proportional counters as the ΔE and silicon surface barrier detectors for the energy measurements. A typical ΔE-E spectrum is shown in Fig. 1.

As one can see, the berilium, boron, and carbon particles emerging from the reactions in the target are clearly separated. We detected the carbon particles ($Z = 6$) from the ^{25}Mg(^{11}B, ^{12}C)^{24}Na proton pickup reaction. This reaction has a positive $Q = +3.893$ MeV and is well separated from the high intensity ^{11}B peaks elastically scattered by the target. The peaks corresponding to the carbon contamination recoiled from the target are seen in the lower energy region of the $Z = 6$ line. Figures 2, 3, and 4 are the energy spectra for the ^{11}B($Z = 5$), carbon ($Z = 6$), and berilium ($Z = 4$) particles.

Our energy resolution of about 200 keV (FWHM) was sufficient to separate the transfer to the ground state ^{25}Mg(^{11}B, ^{12}C)^{24}Na$_{gs}(4^{+})$ from the first doublet of excited states at ^{24}Na$^{m}(1^{+}; 0.472)$ and ^{24}Na$(2^{+}; 0.563)$. The triplet of states at 1.341, 1.345, 1.347 MeV is resolved from the fifth state at $(5^{+}; 1.512)$ although the errors in the determination of the area of the peak for the fifth state are large.

For the ^{25}Mg(^{11}B, ^{10}Be)^{26}Al reaction we resolve the transfer to the ground state ^{26}Al$(5^{+}, 0.0)$ from the first doublet of two excited states ^{26}Al$(3^{+}, 0.42)$ and ^{26}Al$(0^{+}, 0.23)$.

In Figs. 5, 6, and 7 we present the angular distributions for the elastic scattering ^{11}B+^{25}Mg and the transfer reactions.

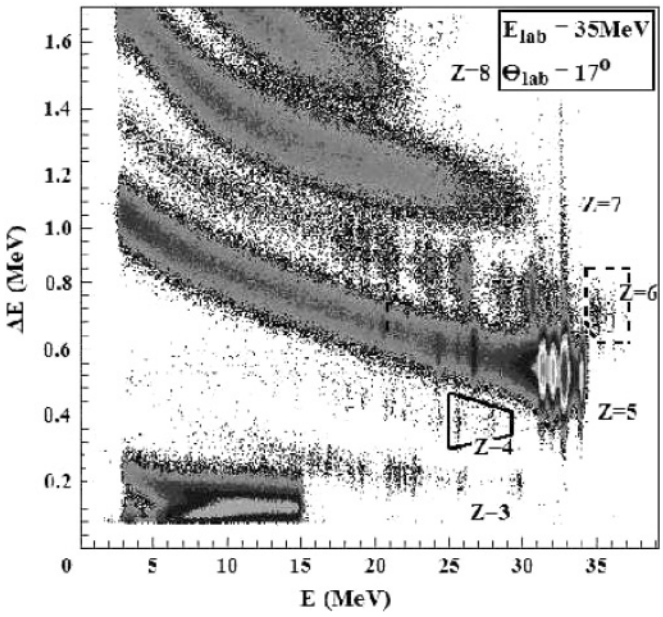

FIG. 1. ΔE-E spectrum. The rectangular and trapezoidal boxes indicate the regions where the peaks of the ^{25}Mg(^{11}B, ^{12}C)^{24}Na and ^{25}Mg(^{11}B, ^{10}Be)^{26}Al reactions appear.

III. DWBA ANALYSIS

The distorted waves used in the DWBA calculations for the entrance and exit channels have been obtained using two different optical potentials, the São Paulo Optical Potential (PSP) [14] and a potential obtained in Ref. [15] (see Table I). In Fig. 5 we present the elastic angular distributions obtained using these two potentials compared to the experimental data. No spin-orbit interaction was taken into account in these calculations.

To determine the spectroscopic factors of the projectile overlap $\langle ^{11}\mathrm{B}|^{12}\mathrm{C}\rangle$ and $\langle ^{11}\mathrm{B}|^{10}\mathrm{Be}\rangle$ we decided to reanalyze data from the literature for the reactions $^{11}\mathrm{B}(d, ^{3}\mathrm{He})^{10}\mathrm{Be}$ [2] and $^{11}\mathrm{B}(d, n)^{12}\mathrm{C}$ [3] using the code fresco. In this reanalysis we firstly used the same optical potentials of Refs. [2,16] for the $d+^{11}$B and ^{3}He$+^{10}$Be channels and the potential of Ref. [17] for the $n + ^{12}$C outgoing channel. The geometry of the bound-state real potentials $p+^{10}$Be, $p+^{11}$B and $d+p$ was fixed to $r_o = 1.25$ fm and $a = 0.65$ fm and the depths were adjusted to reproduce the binding energy of the transfered proton. For the deuteron $p+n$ bound state, two different binding potentials were used: the Reid Soft Core (RSC) tensor potential and a Gaussian form $V_{pn} = -v_0 \exp(-r^2/a^2)$ with $a = 1.484$ fm and $v_0 = 72.15$ MeV [18] but no significant difference between these two was observed. The spectroscopic factors for the projectile were set to $C^2S_{\langle d,n\rangle} = 1$ and $C^2S_{\langle d,^3\mathrm{He}\rangle} = 1.5$ [19].

TABLE I. Optical model parameters used in the DWBA calculations (POT2).

System	V_0	r_0	a_0	W	r_i	a_i	r_c
^{11}B+^{25}Mg	274.0	0.65	0.876	55.8	1.04	0.664	0.6
^{12}C+^{24}Na	274.0	0.75	0.876	55.8	0.7	0.664	0.6

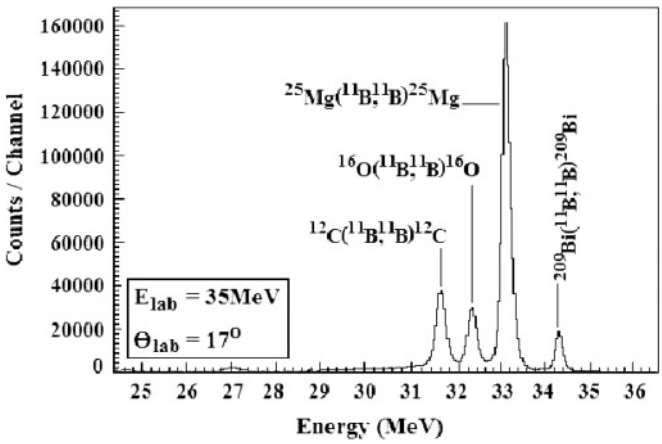

FIG. 2. Energy spectrum for the boron ($Z = 5$). The binning is 40 keV/channel.

With these values for the projectile overlaps we obtained $C^2S_{\langle ^{11}\mathrm{B}|^{12}\mathrm{C}\rangle} = 1.53$, which is about one half of the values of the absolute spectroscopic factors S reported in Refs. [3] and a factor of 4 lower than the Cohen-Kurath [4] value of 5.7 for this overlap. We also performed DWBA calculations for the $^{11}\mathrm{B}(d, n)^{12}\mathrm{C}$ reaction using the PSP in entrance and exit channels. The shape of the transfer angular distribution at forward angles is similar to the one using the optical potentials of Refs. [2,16] but a higher spectroscopic factor of $C^2S = 2.2$ was obtained, going to the direction of the Cohen-Kurath value.

For the $^{11}\mathrm{B}(d, ^{3}\mathrm{He})^{10}\mathrm{Be}$ reaction we obtained $C^2S_{\langle ^{10}\mathrm{Be}|^{11}\mathrm{B}\rangle} = 0.82$ compared to the value of 1.28 reported in Ref. [2] and the Cohen-Kurath value of 0.645 for this overlap.

Finally we decided to use the Cohen-Kurath spectroscopic factors of $C^2S_{\langle ^{11}\mathrm{B}|^{12}\mathrm{C}\rangle} = 5.7$ and $C^2S_{\langle ^{10}\mathrm{Be}|^{11}\mathrm{B}\rangle} = 0.645$ in the further DWBA calculations for the ^{25}Mg(^{11}B, ^{12}C)^{24}Na and ^{25}Mg(^{11}B, ^{10}Be)^{26}Al reactions.

The results of the DWBA calculations are shown in Figs. 6 and 7 and the obtained absolute spectroscopic factors

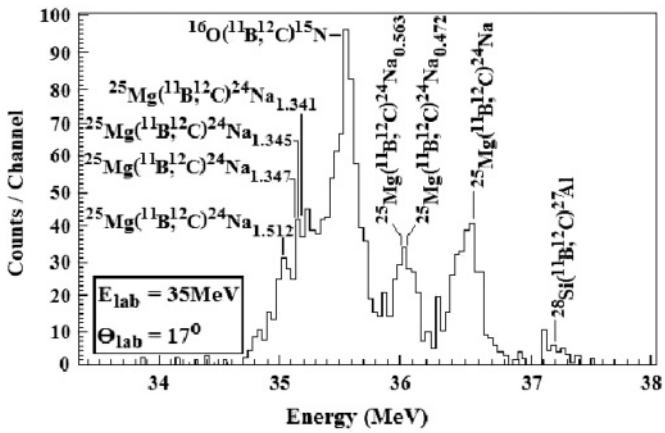

FIG. 3. Energy spectrum for the carbon ($Z = 6$). The binning is 40 keV/channel.

TABLE II. Extracted values for the spectroscopic factors derived from DWBA calculations. C^2S_1 stands for the projectile overlaps $\langle ^{11}\mathrm{B}|^{12}\mathrm{C}\rangle$ and $\langle ^{11}\mathrm{B}|^{10}\mathrm{Be}\rangle$. C^2S_2 stands for the target overlaps.

Reaction	C^2S_1	C^2S_2					
	from [4]	This work		Shell model [7]			Ref. [20]
^{25}Mg(^{11}B,^{12}C)^{24}Na	5.7	PSP	POT2	$2s1/2$	$1d_{3/2}$	$1d_{5/2}$	
^{24}Na$_{gs}$(4$^+$, 0.0)		1.07	0.601		0.075	1.003	1.37
^{24m}Na(1$^+$, 0.472)		0.118	0.118		0.037	0.111	
^{24}Na(2$^+$, 0.563)		0.45	0.268	0.046	0.053	0.363	0.41
^{24}Na(2$^+$, 1.341)		0.0	0.0	0.007	0.008	0.049	
^{24}Na(3$^+$, 1.345)		0.877	0.461	0.043	0.023	0.431	0.58
^{24}Na(1$^+$, 1.347)		0.0	0.0		0.0	0.001	
^{24}Na(5$^+$, 1.512)		0.60	0.322			0.398	0.53
^{25}Mg(^{11}B,^{10}Be)^{26}Al	0.645						Ref. [6]
^{26}Al$_{gs}$(5$^+$, 0.0)		0.302	0.203				0.87
^{26m}Al(0$^+$, 0.23)		0.835	0.593				2.46
^{26}Al(3$^+$, 0.42, $l=0$)		0.208	0.108				0.55
^{26}Al(3$^+$, 0.42, $l=2$)		0.072	0.072				0.0(±0.5)
^{26}Al(1$^+$, 1.06)		0.970	0.655				1.4
^{26}Al(2$^+$, 1.76, $l=2$)		0.524	0.336				0.65

for the overlaps $\langle ^{25}\mathrm{Mg}|^{24}\mathrm{Na}\rangle$ and $\langle ^{25}\mathrm{Mg}|^{26}\mathrm{Al}\rangle$ are listed in Table II. The dashed line corresponds to the DWBA calculations using the São Paulo potential in the entrance and outgoing channels. The solid lines correspond to the calculations using a Wood-Saxon potential whose parameters are given in Table I that we call POT2. Using the POT2 with the modified geometry in the outgoing channel (^{12}C+^{24}Na)) (see Table I), we better reproduced the slope of the transfer angular distributions for the ^{25}Mg(^{11}B, ^{12}C)^{24}Na reaction. To obtain these parameters for the outgoing channel (Table I), a search was performed on the geometry of the imaginary part and we found $r_r = 0.75$ fm and $r_i = 0.7$ fm (Table I).

In all the calculations the two possible representations, post and prior, for the DWBA amplitude were used. The remnant term for the pickup reaction given by $V^{\mathrm{post}}_{\mathrm{remn}} = V_{(^{11}\mathrm{B},^{24}\mathrm{Na})} - U_{(^{12}\mathrm{C},^{24}\mathrm{Na})}$ was taken into account and the difference between post and prior forms was negligible.

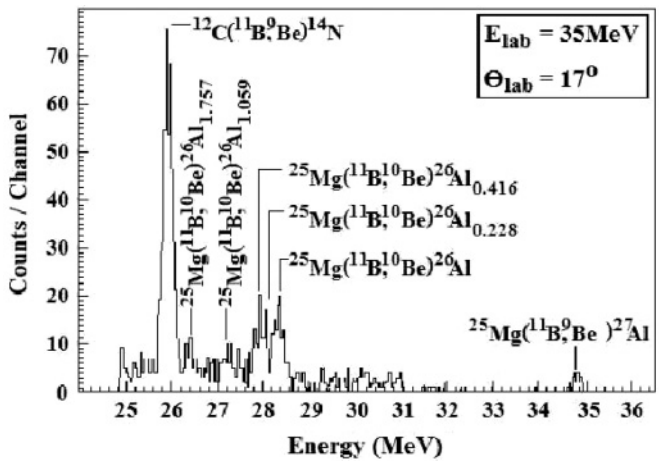

FIG. 4. Energy spectrum for the berilium ($Z = 4$) scattered from the target. The binning is 40 keV/channel.

A. The ^{25}Mg(^{11}B, ^{12}C)^{24}Na reaction

The DWBA calculations for the transfer ^{25}Mg(^{11}B,^{12}C) ^{24}Na reaction were performed considering the proton pickup from the $1d_{5/2}$ state of the target ^{25}Mg. The absolute spectroscopic factors are quoted in Table II. As can be seen from the shell-model spectroscopic factors quoted in Table II the $\langle ^{24}\mathrm{Na}_{gs}|^{25}\mathrm{Mg}\rangle$ overlap is mainly $1d_{5/2}$ with a small contribution of the $1d_{3/2}$ and $1s_{1/2}$ states. The spectroscopic

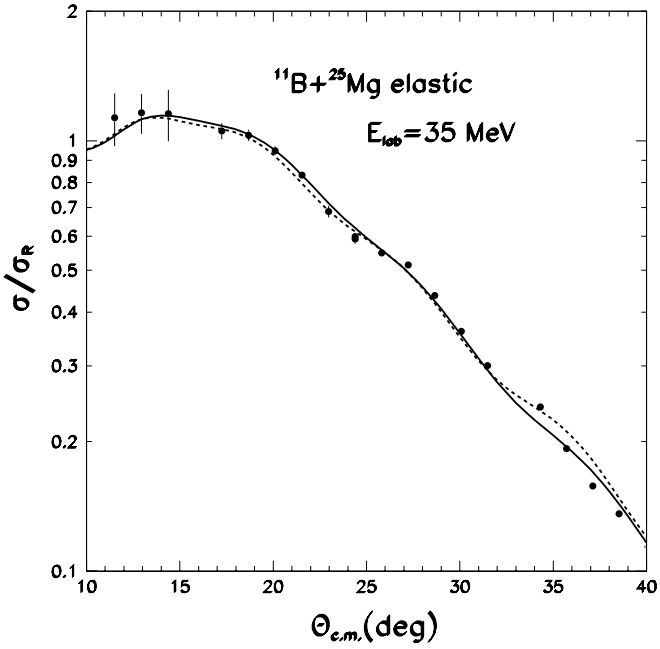

FIG. 5. Elastic scattering of ^{11}B+^{25}Mg at $E_{\mathrm{lab}} = 35$ MeV and ^{25}Mg(^{11}B, ^{12}C)^{24}Na reaction. The dashed line is the OM calculation using the São Paulo potential and the solid line is obtained with the potential of Table I for the ^{11}B+^{25}Mg.

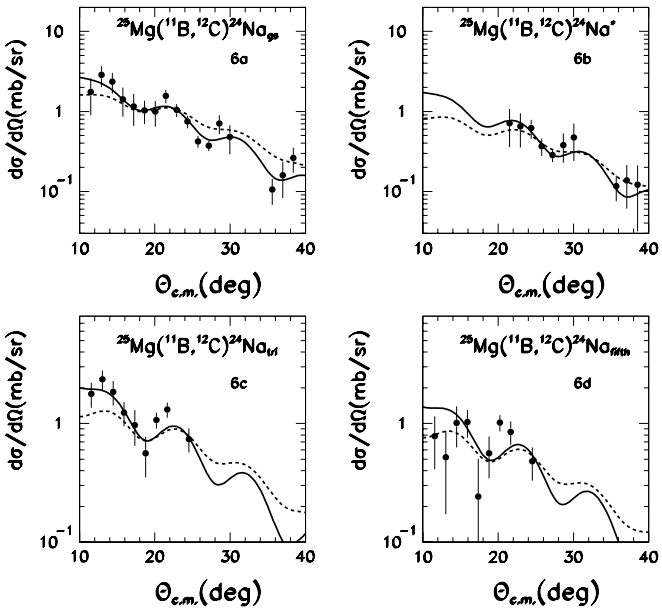

FIG. 6. Elastic scattering of ^{11}B+^{25}Mg at $E_{\rm lab} = 35$ MeV and ^{25}Mg(^{11}B, ^{12}C)^{24}Na reaction. Dashed line is the DWBA calculation using the São Paulo potential and the solid line using the parameters of Table I for the entrance and exit channels. Details are given in the text.

factor for the ground state is consistent with the shell-model predictions from Ref. [7] except for the ground state with POT2, which is a factor of 2 lower than the shell-model prediction. For the first two excited states of the ^{24}Na at 0.472 and 0.563 MeV [(Fig. 6(b)] our data provide only a test of consistency between our spectroscopic factors and those from the shell model because our energy resolution was not sufficient to resolve the two states. In Fig. 6(b) the solid line is the sum of the cross section for the isomeric state at 0.472 MeV using the shell-model spectroscopic factor for $1d_{5/2}$ (see Table II) and the 0.563-MeV level whose spectroscopic factor was varied to reproduce the magnitude of the cross section.

For the triplet of states 1.341, 1.345, 1.347 [Fig. 6(c)] the shell-model calculations predict that the main contribution comes from the state 1.345($1d_{5/2}$). In our DWBA calculations we considered only this state and the spectroscopic factor obtained using potential POT2 agrees well with the shell-model prediction (see Table II). The spectroscopic factor using PSP is about a factor of 2 larger than the shell-model calculations for this level. The spectrosocpic factors obtained for the excited state at 1.512 MeV [Fig. 6(d)] are in relatively good agreement with shell-model predictions and previous measurements.

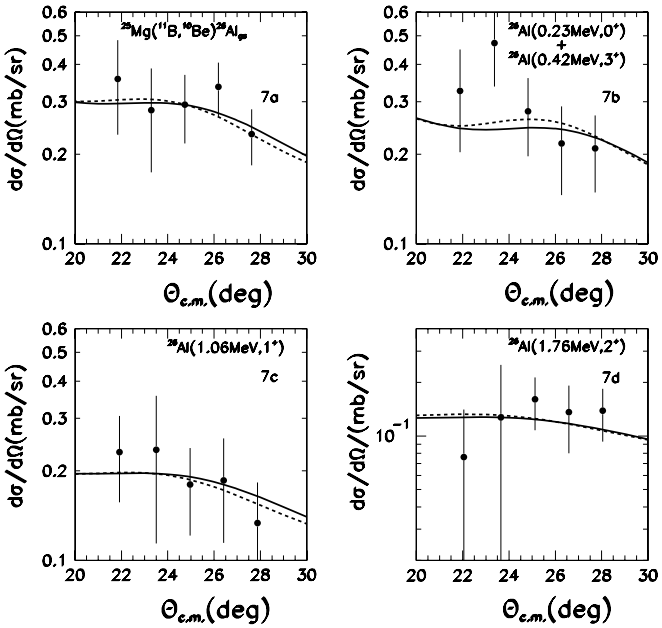

FIG. 7. ^{25}Mg(^{11}B, ^{10}Be)^{26}Al reaction. Dashed line is the calculation with the São Paulo potential and the solid line using the potential parameters of Table I for ^{11}B+^{25}Mg in both entrance and exit channels.

B. The ^{25}Mg(^{11}B, ^{10}Be)^{26}Al reaction

The shape of the angular distributions of the stripping reaction ^{25}Mg(^{11}B, ^{10}Be)^{26}Al is reasonably reproduced by the DWBA calculations with both optical potentials as can be seen in Fig. 7. However the spectroscopic factors obtained for the $\langle ^{26}\mathrm{Al}|^{25}\mathrm{Mg}\rangle$ overlap are lower than the values previously reported in the literature from ^{25}Mg(d, n) [5] and ^{25}Mg(^{3}He, d) [6] measurements. In Refs. [5,6], a discrepancy of a factor of 2 in the relative spectroscopic factors between the ^{25}Mg(^{3}He, d)^{26}Al and ^{25}Mg(d, n) measurements is reported, the $\langle d, n\rangle$ being lower. Our measurements provided an absolute spectroscopic factor for the ground state of ^{26}Al [Fig. 7(a)] that is about a factor of 3–4 lower than the $\langle ^3\mathrm{He}, d\rangle$ measurements (see Table II), depending on the optical potential used in the calculation. The analysis of the angular distribution of the first two excited states of ^{26}Al [Fig. 7(b)] was made by summing the contributions of the first excited isomeric state ^{26m}Al(0^+, 0.23) and the second excited state ^{26}Al(3^+, 0.42) with contributions from $l = 0$ and $l = 2$ components. The spectroscopic factors for these two excited states quoted in Table II were adjusted by keeping approximately the same ratio of $S_{\rm exct}/S_{\rm gs}$ from Ref. [6] for these states (see Table II). For the ^{26}Al(2^+, 1.76) excited state we considered only $l = 2$ contribution because our data are not sensitive to the different shapes of the angular distributions for the $l = 0$ and $l = 2$ contributions in this angular range.

We performed CCBA calculations considering the transfer ^{24}Mg(^{11}B, ^{10}Be)^{26}Al reaction followed by the excitation of the ^{26}Al and taking into account the coupling between the four first excited states of the ^{26}Al. A proton-^{25}Mg structure is assumed for the ^{26}Al with potentials for the proton-^{25}Mg and the core-core ^{10}Be-^{25}Mg being folded together to give the optical potential in the outgoing channel. However, the effect of the coupling was found to be of a few percentages and does not explain the discrepancies observed in the spectroscopic factors. We also performed CRC calculations considering the transfer to all orders and the effect was found to be negligible in the angular range of our measurements.

IV. SUMMARY

We measured angular distributions for the elastic scattering ^{11}B+^{25}Mg at $E_{^{11}\mathrm{B}} = 35$ MeV, the proton pickup ^{25}Mg(^{11}B, ^{12}C)^{24}Na, and the stripping ^{25}Mg(^{11}B, ^{10}Be)^{26}Al transfer reactions leading to the ground state and excited states of the ^{24}Na and ^{26}Al nuclei. The angular distributions have been analyzed using DWBA calculations and the spectroscopic factors have been obtained. For the ^{25}Mg(^{11}B, ^{10}Be)^{26}Al reaction, the spectroscopic factors are lower than the values reported in the literature obtained from ^{25}Mg(d, n) and ^{25}Mg(^{3}He, d) reactions. CCBA calculations considering the coupling to excited states of ^{26}Al were performed and do not account for the observed discrepancies. The results for the $\langle ^{25}\mathrm{Mg}|^{24}\mathrm{Na}\rangle$ overlap are in good agreement with the spectroscopic factors obtained from shell-model calculations and previous measurements.

ACKNOWLEDGMENTS

The authors thank FAPESP for the financial support (Projeto Temático 01/06676-9).

[1] I. J. Thompson, Comput. Phys. Rep. **7**, 167 (1988).
[2] W. Fitz, R. Jahr, and R. Santo, Nucl. Phys. **A101**, 449 (1967).
[3] G. H. Neuschaefer, M. N. Stephens, S. L. Tabor, and K. W. Kemper, Phys. Rev. C **28**, 1594 (1983).
[4] S. Cohen and D. Kurath, Nucl. Phys. **A101**, 1 (1967).
[5] H. Fuchs *et al*., Nucl. Phys. **A110**, 65 (1968).
[6] A. Weidinger, R. Siemssen, G. Morrison, and B. Zeidman, Nucl. Phys. **A108**, 547 (1968).
[7] J. Vernotte, G. Berrier-Ronsin, S. Fortier, E. Hourani, J. Kalifa, J. M. Maison, L. H. Rosier, G. Rotbard, and B. H. Wildenthal, Phys. Rev. C **57**, 1256 (1998).
[8] R. Lichtenthaler, A. Lépine-Szily, V. Guimarães, G. Lima, and M. Hussein, Eur. Phys. J. A **25**, 733 (2005).
[9] I. A. Kondurov, E. M. Korotkikh, Y. V. Petrov, and G. I. Shuljak, Phys. Lett. **B106**, 383 (1981).
[10] F. D. Becchetti, *et al*., Phys. Rev. C **42**, R801 (1990).
[11] M. Y. Lee, F. D. Bechetti, T. W. O'Donnell, D. A. Roberts, J. A. Zimmerman, J. J. Kolata, V. Guimarães, D. Peterson, P. Santi, P. A. DeYoung *et al*., Nucl. Instrum. Methods Phys. Res. A **422**, 536 (1999).
[12] F. D. Bechetti, M. Y. Lee, T. W. O'Donnell, D. A. Roberts, J. J. Kolata, L. O. Lamm, G. Rogachev, V. Guimarães, P. A. DeYoung, and S. Vincent, Nucl. Instrum. Methods Phys. Res. A **505**, 377 (2003).
[13] N. Ueta and W. G. P. Engel, Nucl. Instrum. Methods Phys. Res. A **282**, 185 (1989).
[14] L. C. Chamon, B. V. Carlson, L. R. Gasques, D. Pereira, C. De Conti, M. A. G. Alvarez, M. S. Hussein, M. A. Cândido Ribeiro, E. S. Rossi, and C. Silva, Phys. Rev. C **66**, 014610 (2002).
[15] P. N. de Faria, Master's Thesis, Instituto de Física da USP, 2003.
[16] G. S. Mutchler, D. Rendic, D. E. Velkley, W. E. Sweeney, and G. C. Phillips, Nucl. Phys. **A172**, 469 (1971).
[17] At. Data Nucl. Data Tables **17**, 1 (1976).
[18] M. Assunção, R. Lichtenthaler, V. Guimarães, A. Lépine-Szily, G. F. Lima, and A. M. Moro, Phys. Rev. C **70**, 054601 (2004).
[19] R. H. Bassel, Phys. Rev. **149**, 791 (1966).
[20] E. Kraemer and G. Mairle, Kaschl, Nucl. Phys. **A165**, 353 (1971).